

An Auxin Gradient and Maximum in the *Arabidopsis* Root Apex Shown by High-Resolution Cell-Specific Analysis of IAA Distribution and Synthesis ^W

Sara V. Petersson,^a Annika I. Johansson,^a Mariusz Kowalczyk,^a Alexander Makoveychuk,^a Jean Y. Wang,^b Thomas Moritz,^a Markus Grebe,^c Philip N. Benfey,^b Göran Sandberg,^c and Karin Ljung^{a,1}

^a Department of Forest Genetics and Plant Physiology, Umeå Plant Science Centre, Swedish University of Agricultural Sciences, SE-901 83 Umeå, Sweden

^b Department of Biology and Institute for Genome Sciences & Policy, Center for Systems Biology, Duke University, Durham, North Carolina 27708, USA

^c Department of Plant Physiology, Umeå Plant Science Centre, Umeå University, SE-901 87 Umeå, Sweden

Local concentration gradients of the plant growth regulator auxin (indole-3-acetic acid [IAA]) are thought to instruct the positioning of organ primordia and stem cell niches and to direct cell division, expansion, and differentiation. High-resolution measurements of endogenous IAA concentrations in support of the gradient hypothesis are required to substantiate this hypothesis. Here, we introduce fluorescence-activated cell sorting of green fluorescent protein-marked cell types combined with highly sensitive mass spectrometry methods as a novel means for analyses of IAA distribution and metabolism at cellular resolution. Our results reveal the presence of IAA concentration gradients within the *Arabidopsis thaliana* root tip with a distinct maximum in the organizing quiescent center of the root apex. We also demonstrate that the root apex provides an important source of IAA and that cells of all types display a high synthesis capacity, suggesting a substantial contribution of local biosynthesis to auxin homeostasis in the root tip. Our results indicate that local biosynthesis and polar transport combine to produce auxin gradients and maxima in the root tip.

INTRODUCTION

The growth-regulating substance indole-3-acetic acid (IAA) is essential for normal plant growth and development and for responses to environmental factors, such as light and gravity. It has long been believed that auxin acts through the development of gradients and concentration maxima within developing tissues and that these gradients provide positional cues for diverse developmental processes (Bhalerao and Bennett, 2003; Leyser 2006; Prusinkiewicz and Rolland-Lagan, 2006; Tanaka et al., 2006; Benjamins and Scheres, 2008; Ikeda et al., 2009).

Although most tissues display some IAA synthesis capacity, IAA is predominantly synthesized in young, developing tissues, such as the apical parts of roots and the base of developing leaves (Ljung et al., 2001). Symplastic polar transport of IAA redistributes IAA within these organs and throughout the plant (Blakeslee et al., 2005). There is also evidence for phloem transport of IAA from the shoot to the root system (Swarup et al., 2001). IAA can be catabolized or conjugated to various amino acid and sugar moieties, enabling a reduction of the levels

of active hormone and reversible or irreversible storage (Woodward and Bartel, 2005).

In most developmental studies on the role of auxin, of which many have been performed in the *Arabidopsis thaliana* root apex (Benfey and Scheres, 2000), different indirect methods of assessing IAA distributions have been used. These include analyses of various IAA-responsive promoters or promoter elements driving the expression of β -glucuronidase (GUS) or green fluorescent protein (GFP) markers (Ulmasov et al., 1997; Sabatini et al., 1999; Ottenschläger et al., 2003; Swarup et al., 2005), transport patterns of radio labeled auxins (Chen et al., 1998), and immunolocalization studies with antibodies raised against IAA (Caruso et al., 1995; Benková et al., 2003).

Here, we describe the direct quantification of IAA in specific cell types of the *Arabidopsis* root apex by a combination of fluorescence-activated cell sorting (FACS) and mass spectrometry-based IAA quantification and biosynthesis measurements. This approach complements the similar approach used to generate a transcriptional expression map of the *Arabidopsis* root at cell type-specific resolution (Birnbaum et al., 2003, 2005; Brady et al., 2007) and opens new avenues for cell type-specific analyses of diverse molecules regulating development of multicellular organisms.

Data from 14 different GFP-expressing lines were combined to produce a map of IAA distribution in the *Arabidopsis* root tip. The analyses identified the sites of high synthesis capacity in the root tip and clearly demonstrated the presence of an IAA

¹ Address correspondence to karin.ljung@genfys.slu.se.

The author responsible for distribution of materials integral to the findings presented in this article in accordance with the policy described in the Instructions for Authors (www.plantcell.org) is: Karin Ljung (karin.ljung@genfys.slu.se).

^W Online version contains Web-only data.

www.plantcell.org/cgi/doi/10.1105/tpc.109.066480

concentration gradient within the root, with a clear maximum in the quiescent center (QC) of the root apex.

RESULTS

Quantification of IAA in Isolated Protoplasts

To validate our method, we performed a series of control experiments to show that the concentration of IAA in isolated protoplasts produces a valid measurement of endogenous IAA levels. To obtain free protoplasts for cell sorting and subsequent IAA analysis, the cell walls were removed by incubating *Arabidopsis* roots in a medium containing cell wall-degrading enzymes. Isolated protoplasts were then sorted by FACS into GFP-expressing and non-GFP-expressing cell populations (see Methods). To examine the possible effects of isolating and sorting protoplasts on leakage and/or IAA metabolism, we performed a number of control experiments.

First, we analyzed the effects of various IAA transport inhibitors on the cellular IAA contents of isolated protoplasts by adding naphthylphthalamic acid (NPA), 1-naphthoxyacetic acid (1-NOA), NPA + 1-NOA, or sodium azide (NaN_3) to the protoplast isolation

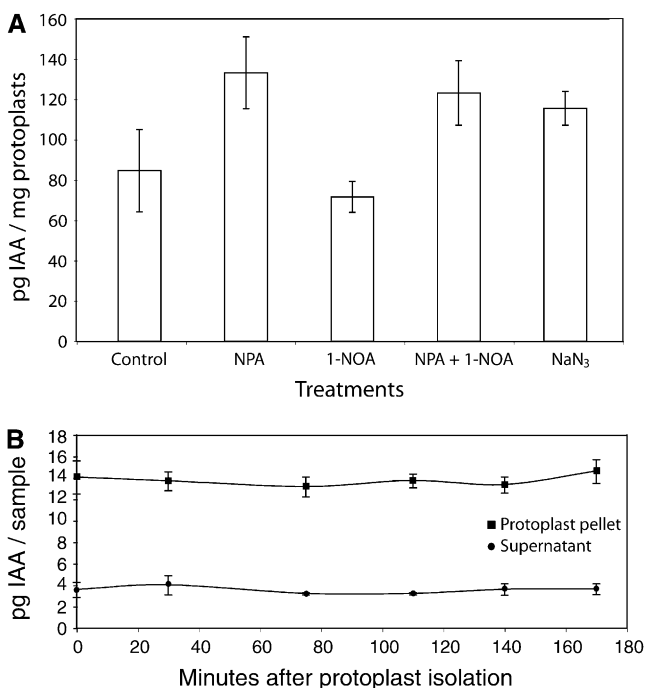


Figure 1. IAA Concentrations in Isolated Protoplasts.

(A) IAA concentrations after treatment with or without the transport inhibitors NPA, 1-NOA, NPA + 1-NOA, or NaN_3 during protoplast isolation, normalized to pg IAA/mg protoplasts based on average cell volumes (see Figure 2A).

(B) IAA concentrations in isolated protoplasts and in the PBS sorting buffer during simulated sorting for up to 170 min. Each sample consisted of 150,000 isolated protoplasts. Samples were analyzed in triplicate, and error bars indicate SD.

Table 1. Change in IAA Concentration in Sorted Cells after NPA Treatment

	GFP - NPA	GFP + NPA	Ref - NPA	Ref + NPA
M0028	1	17.50%	1	18.20%
<i>pWOL::GFP</i>	1	-9.60%	1	2.90%
J2812	1	-19.90%	1	4.1%
<i>pSCR::GFP</i>	1	-16.50%	1	-16.30%
<i>PET111::GFP</i>	1	-7.40%	1	21.90%

Five *Arabidopsis* lines expressing GFP in specific cell types of the root were used for this experiment. Roots from seedlings 8 d after germination were treated with and without NPA during protoplast isolation. After sorting, IAA was quantified in the GFP and in the reference cell population, respectively. The IAA concentration in the GFP positive population (GFP - NPA) and in the reference population (Ref - NPA) was set to 1 for the seedlings untreated with NPA. For the + NPA conditions, the percentage of change in IAA concentration relative to the appropriate control population (GFP or Ref) is shown. For these five lines, adding NPA to the isolation buffer does not significantly change the IAA concentration in sorted cells.

medium (Figure 1A). Blocking IAA efflux with NPA (Blakeslee et al., 2005; Petrasek et al., 2006) resulted in 40% higher IAA contents in the isolated cells, while treatment with 1-NOA to prevent IAA influx (Parry et al., 2001) did not cause any significant changes in IAA content compared with the untreated controls. Treatment with a combination of NPA and 1-NOA gave the same results as treatment with NPA alone, while treatment with NaN_3 to block energy-dependent metabolic and membrane transport processes (Wright and Oparka, 1997) resulted in a 40% increase in IAA content in isolated cells, comparable to that induced by the NPA treatment (Figure 1A). We also analyzed the effect of NPA treatment on the cellular IAA concentration in sorted protoplasts from five *Arabidopsis* lines, expressing GFP in specific cell types of the root apex (M0028, *pWOL::GFP*, J2812, *pSCR::GFP*, and *PET111::GFP*; see Supplemental Table 1 and Supplemental Figure 1 online for descriptions of the GFP expression patterns). For all tested GFP expressing lines, treatment with NPA during protoplast isolation did not cause any significant changes in IAA concentration in the sorted cells (Table 1), although there were large differences in the intracellular IAA concentration between these lines.

Second, to assess the extent to which potential IAA leakage from isolated protoplasts might occur over time, we simulated the sorting procedure by suspending isolated protoplasts in PBS sorting buffer at 4°C and analyzed the IAA concentrations in both the protoplasts and the buffer over 170 min. As shown in Figure 1B, no significant leakage of IAA from isolated protoplasts was detected during the simulated sorting procedure. The PBS buffer initially contained a low amount of IAA that probably originated from residual cell wall debris, but the IAA concentration in the buffer did not increase over time. In otherwise identical experiments in which NPA was added to the isolation buffer to block IAA efflux from the cells, the initial IAA concentration in the isolated protoplasts was slightly higher, but again we did not detect any significant leakage from the isolated protoplasts. Very little is known about the effect of cell wall-degrading enzymes on the activity of the IAA influx and efflux carriers. It is very likely that

the protoplasting procedure changes the efficiency of these transporters, thereby causing changes in IAA influx and efflux and most likely a lowering of the IAA transport rate. The fact that we could not detect any significant leakage from the isolated protoplasts during simulated sorting suggests that they have much lower IAA transport competence than cells in planta.

Third, we obtained metabolite profiles from samples of isolated protoplasts that had been incubated with or without NPA or NaN_3 during their isolation. The samples were analyzed by gas chromatography–time of flight–mass spectrometry, and principal component analysis (PCA) of the resulting data, processed according to Jonsson et al. (2005), did not reveal any significant treatment-related separations (see Supplemental Figure 2 online). Thus, treatment with IAA transport inhibitors during the isolation procedure did not appear to cause any significant changes in the metabolite profile.

Finally, to examine whether any changes in IAA catabolism were induced by the isolation procedure, we performed a feeding experiment in which radioactively labeled IAA was applied to both whole *Arabidopsis* seedlings and to intact roots. The metabolite profile obtained after feeding whole seedlings with radioactively labeled IAA corresponded to previous findings by Östin et al. (1998). When applied to the cut surface of intact roots,

exogenous IAA was quickly transported down through the root system and metabolized, mainly to 2-oxoindole-3-acetic acid and 2-oxoindole-3-acetyl- β -D-glucopyranose. The 2-oxoindole-3-acetic acid was also the major catabolite observed in isolated protoplasts, while IAA conjugates were formed in minor amounts. Radioactivity profiles of IAA metabolites in whole seedlings, intact roots, and isolated root protoplasts were very similar, indicating that the protoplast isolation procedure did not cause significant changes in IAA catabolism and conjugation.

Taken together, these data show that very little leakage of IAA occurred from isolated protoplasts and that IAA metabolism was not significantly affected by the protoplast isolation procedure. Data from previous studies indicate that NaN_3 treatment may have differing effects on different transport mechanisms and that NaN_3 may change cells' physical properties (Tucker, 1993; Wright and Oparka, 1997). Different cell types may also respond differently to treatments with transport inhibitors, such as NPA and 1-NOA (Blakeslee et al., 2005; Petrusek et al., 2006). We therefore decided to add neither IAA transport inhibitors nor NaN_3 during the protoplast isolation procedure. Instead, we optimized the procedure and minimized the time the cells were kept on ice prior to sorting to minimize any strain on the protoplasts.

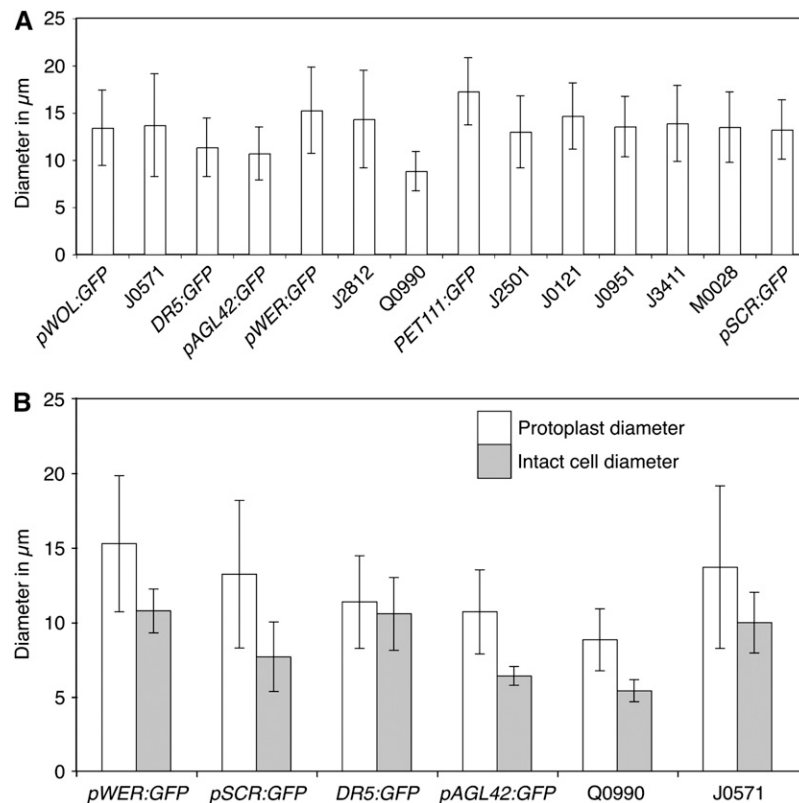


Figure 2. Protoplast and Cell Diameters of Different Cell Types of the *Arabidopsis* Root.

(A) Average diameters of GFP expressing protoplasts isolated from the different GFP lines used in this study.

(B) Cell diameter in relation to protoplast diameter for each of six GFP lines. Diameters of intact cells were calculated from cell volume measurements made on intact roots. Samples were analyzed in triplicate, and error bars indicate SD ($n = 10$).

Cell Size Measurements and Data Normalization

Protoplasts isolated from root tissue of *Arabidopsis* lines expressing GFP in specific cell types of the root tip were sorted by FACS into GFP-expressing cells and nonexpressing cells, thus obtaining a specific reference population for each biological replicate. After sample extraction and purification, IAA was quantified using gas chromatography–selected reaction mode–mass spectrometry (GC–SRM–MS) (see Methods).

Since each technical replicate consisted of a known but variable number of protoplasts (usually $\sim 150,000$ to $200,000$) of different sizes, we normalized their IAA concentrations according to their weight, calculated from size measurements, as follows. First, the diameter of the GFP-expressing protoplasts was measured using light microscopy, and the average cell size for each line was calculated (Figure 2A). The volume and finally the weight of the protoplasts were then calculated from their average diameters, assuming that cells of all types had an equal density, equivalent to that of water. Immediately after protoplast isolation, the volume of the cells showed an expected initial, rapid increase. Subsequently, however, the volumes remained constant, facilitating an accurate cell volume determination for comparison between the different cell lines. Consistent with these findings, protoplasts obtained from roots of horseradish seedlings have previously been reported to swell to maximal sizes within a minute in a 450 mM sorbitol solution. Both cortical and endodermal root cells were analyzed, and no variation due to cell type was observed (Suga et al., 2003).

Second, the volumes of the intact GFP-expressing cells were also calculated, from a z-stack of confocal laser scanning microscopy (CLSM) images. Cell volume data obtained from the CLSM images were converted to diameters of hypothetical spheres and compared with the protoplast diameters to investigate whether protoplasts of different cell types displayed different degrees of expansion in the isolation buffer. As shown in Figure 2B, the increases in protoplast diameters were proportional to the diameters of the intact cells.

The average number of protoplasts of each line required for a total calculated mass of 1 mg (6×10^5 to 2.7×10^6 cells, depending on the line) was multiplied by the measured IAA concentration per protoplast, giving the IAA concentration in each line in terms of pg IAA/mg protoplasts. The IAA concentration in each GFP-expressing protoplast population was then divided by the IAA concentration in the respective reference population. In the IAA distribution maps, the IAA concentration is shown relative to the concentration in the internal reference population for each cell line, which consists of all non-GFP-expressing cells from the same samples. From these data we have also calculated the intracellular IAA concentration to be in the range of 1 to 50 μM in cells coming from the most apical millimeter of the root.

The normalization procedure assumes that IAA is evenly distributed within the cell. Unfortunately, there is little published data on the subcellular distribution of IAA and IAA metabolites in any plant species, even though localization studies suggest that many enzymes believed to be involved in IAA synthesis downstream of Trp are located to the cytoplasm, while Trp biosynthesis is plastidic (Woodward and Bartel, 2005). Active transport

of IAA and IAA metabolites between cellular compartments is likely to be very important in regulation of subcellular IAA homeostasis. There is data suggesting that a substantial part (~ 30 to 40%) of the intracellular IAA pool within tobacco (*Nicotiana tabacum*) and Scots pine (*Pinus sylvestris*) leaves is located to the chloroplasts (Sandberg et al., 1990), but the role of plant vacuoles for IAA storage and turnover is currently unclear. Since vacuoles take up a proportionally larger part of the cell volume in some cell types compared with others, this could affect the normalized values.

Mapping the IAA Distribution in the *Arabidopsis* Root Apex

We combined quantitative data from 14 different GFP-expressing *Arabidopsis* lines (see Supplemental Table 1 and Supplemental Figure 1 online) to construct the IAA distribution map in Figure 3 as follows. Seedlings were grown on agar under long-day conditions for 8 d, and their roots were harvested and pooled for protoplast isolation, cell sorting, and IAA quantification. Data were acquired from four to six biological replicates, each consisting of at least three technical replicates, except for the QC line

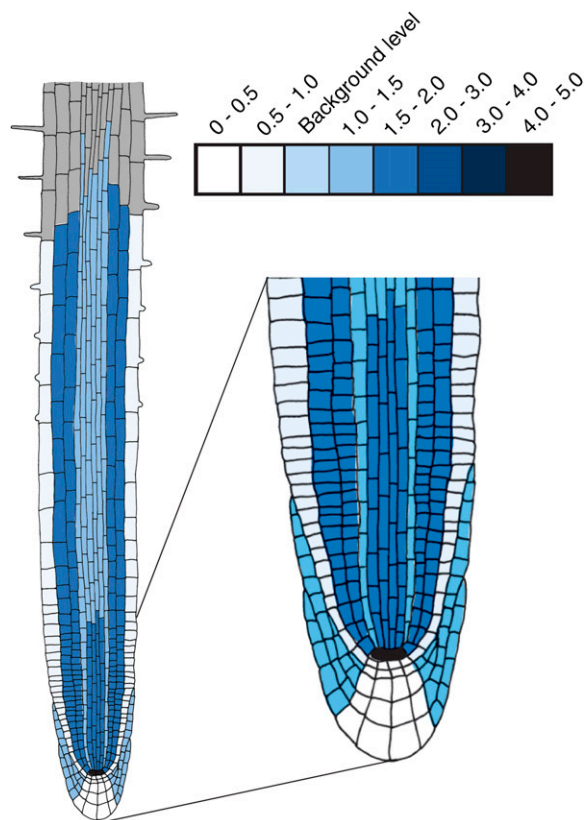


Figure 3. IAA Distribution within the *Arabidopsis* Root Apex.

The data presented in the figure were derived from 14 GFP lines covering all of the different cell types of the root apex. Cell type–specific IAA concentrations were calculated relative to those in the reference population for each GFP cell line, and the color scale indicates the IAA concentration relative to this reference population.

pAGL42:GFP, for which pooled material from eight biological replicates was employed. Instead of making direct comparisons between cell lines, the data were normalized against their respective internal reference protoplast populations to compensate for slight differences in growth rate and development between biological replicates and between different GFP-expressing *Arabidopsis* lines.

The highest relative IAA concentration, fivefold higher than the concentration in the surrounding root tissue, was observed in the QC cells. The cortex, endodermis, and apical parts of the stele contained twice as much IAA as the average surrounding tissue. The columella and epidermis, on the other hand, had lower IAA levels than average in the surrounding tissue.

The data for the individual lines presented in Figure 4A fully support the IAA distribution map shown in Figure 3, indicating that a gradient in IAA concentration is present in the stele, with IAA levels increasing toward the root apex in all of the lines J2501, *pWOL:GFP*, and Q0990 (Figure 4A), even though J2501 and *pWOL:GFP* do not contain QC cells, while Q0990 does. Since the QC cells contain very high IAA levels, it is difficult to determine whether the very high IAA concentrations in Q0990 reflect further increases in IAA concentration toward the apex, compared with *pWOL:GFP* and J2501, or are caused by the QC cells. The occurrence of an IAA gradient toward the apical region of the root has previously been demonstrated between root sections in the millimeter range (Bhalerao et al., 2002; Ljung et al.

2005). This observation can now be corroborated and refined with our present cell type-specific IAA measurements.

The data from the QC line *pAGL42:GFP* are based on data from eight pooled biological samples, since it was difficult to collect sufficiently large amounts of GFP-positive cells from this line. As shown in Figure 4B, the IAA concentration observed within these cells is very high. The IAA concentrations in the GFP-expressing cells of the *DR5:GFP* and M0028 lines (which possess QC cells) are also high relative to the concentrations in their reference populations. On the other hand, the IAA concentration in the GFP-expressing cells of the columella line *PET111:GFP* (which does not contain QC cells) is lower than in the reference population. Lateral root cap cells are represented by the GFP-expressing cells of the lines M0028 and J0951. Since GFP is also expressed in QC cells of line M0028, the results obtained from the J0951 line are likely to most accurately reflect the IAA concentration in lateral root cap cells.

All Cell Types within the Root Apex Show Elevated IAA Biosynthesis Rates

The data compiled in Figure 3 suggest that substantial concentrations of IAA accumulate in the QC as well as in the apical parts of the stele, cortex, and endodermis. To assess the role of de novo IAA synthesis in the formation of this gradient, we analyzed IAA synthesis rates in specific cell types of the root apex. Four

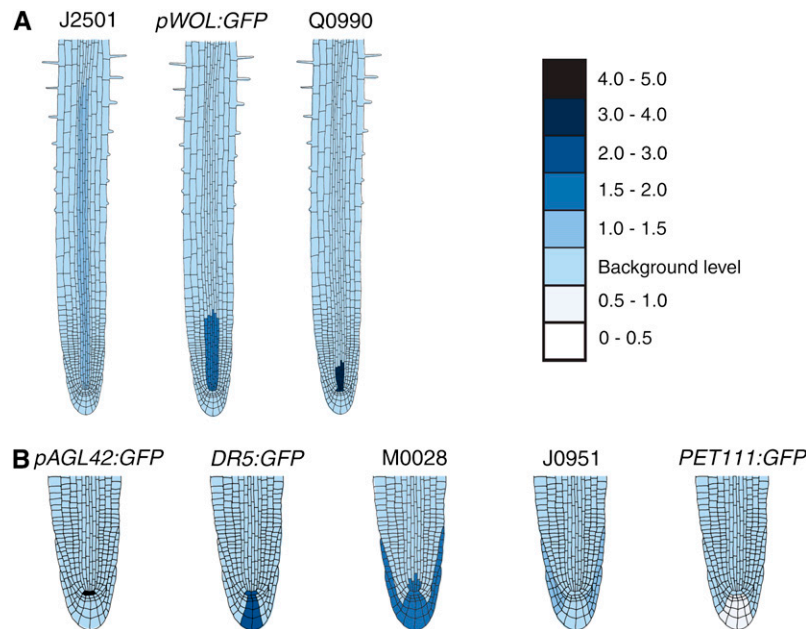


Figure 4. IAA Distributions in Specific Stele and Root Cap *Arabidopsis* GFP Lines.

(A) Increases in IAA concentrations toward the root apex can be observed in the stele in lines J2501, *pWOL:GFP*, and Q0990. The extent to which the high IAA level in Q0990 is due to a high IAA concentration in the stele initials or the very high concentration of IAA within its QC cells is unclear.

(B) IAA concentration in QC cells, columella initials, columella cells, and in the lateral root cap. The QC cells show a fivefold increase in IAA concentration compared with the reference population, according to both direct measurements on the QC line *pAGL42:GFP* and measurements on the lines *DR5:GFP* and M0028 (expressing GFP in the QC), which show four- and threefold higher concentrations compared with their reference populations, respectively. By contrast, IAA concentrations in the J0951 and *PET111:GFP* lines, which do not contain GFP-expressing QC cells, are similar or lower than those in the reference populations.

GFP-expressing lines (J2812, *pSCR:GFP*, *pWOL:GFP*, and M0028) that together cover all the different cell types within the root apex were used in this experiment (Figure 5A). The aerial parts of seedlings were removed at day eight after germination, prior to incubation with labeled tracer, to prevent transport of newly synthesized IAA from the shoot to the root. The excised roots were then incubated in medium containing 30% deuterium oxide and 40 μ M NPA for 16 h. In this case, NPA was added to prevent transport of newly synthesized IAA out of the root cells. Protoplasts were isolated from the roots and sorted by FACS, and IAA biosynthesis rates were analyzed by GC-SRM-MS (Ljung et al., 2005).

The GFP-positive cells from all four lines showed higher IAA synthesis rates than background levels (Figure 5B), but there were no indications that synthesis rates were significantly higher in any of the examined tissues when compared with the others. The reference population consisted mostly of cells located above the apex, while the GFP-positive protoplast populations originated mainly from the most apical 0.5-mm section of the primary root tip. These findings corroborate previous data indicating that the IAA synthesis rate may be highest in the most apical section of the primary root (Ljung et al., 2005).

DISCUSSION

We have successfully developed a method for IAA analysis from small numbers of cells of specific cell types using cell sorting of GFP-expressing *Arabidopsis* lines followed by sensitive MS-based IAA measurements. Using this technique, cell-specific IAA quantification and biosynthesis measurements were possible from lines with GFP expression in as few as four to seven cells per root (*pAGL42:GFP*, QC cell expressing line) (Nawy et al., 2005).

Previously, the only plant tissues in which auxins have been able to be measured at near-cellular resolution are the wood-forming tissues of various tree species, where gradients of IAA concentrations, with maxima in the cambial stem cells, have been observed after cryosectioning of the samples followed by MS analyses (Uggla et al., 1996).

Here, we selected 14 transgenic *Arabidopsis* lines that collectively express GFP in all cell types of the primary root apex. The lines were selected because they provided the most cell type-specific expression patterns available. Some of these lines display partially overlapping expression patterns. This feature was exploited to confirm the IAA measurements performed on the epidermal, cortical, endodermal, and pericycle cell layers.

The IAA distribution map presented here unequivocally reveals the existence of a gradient of IAA concentration within the root apex, with the highest IAA concentration occurring in the QC cells. Relatively high IAA concentration was also observed in the cortex, endodermis, and apical parts of the stele, while the columella and epidermis showed lower levels than the average. Data from cell type-specific gene expression analysis has shown that several genes related to auxin responses are highly expressed in the stele (Birnbaum et al., 2003). In another data set, some putative auxin biosynthesis genes were transcriptionally enriched in the QC, lateral root primordia, and pericycle. Auxin conjugating enzymes showed an enriched expression in the columella, while the expression of auxin transporters was enriched in the columella, hair cells, and cortex (Brady et al., 2007). This indicates that there is a correlation between the expression patterns of many IAA-related genes and the IAA distribution map. It is particularly intriguing that expression of genes that are known to be downregulating IAA concentrations show such a strong expression in the columella, suggesting that the relatively low levels of IAA in this cell type might be caused by a

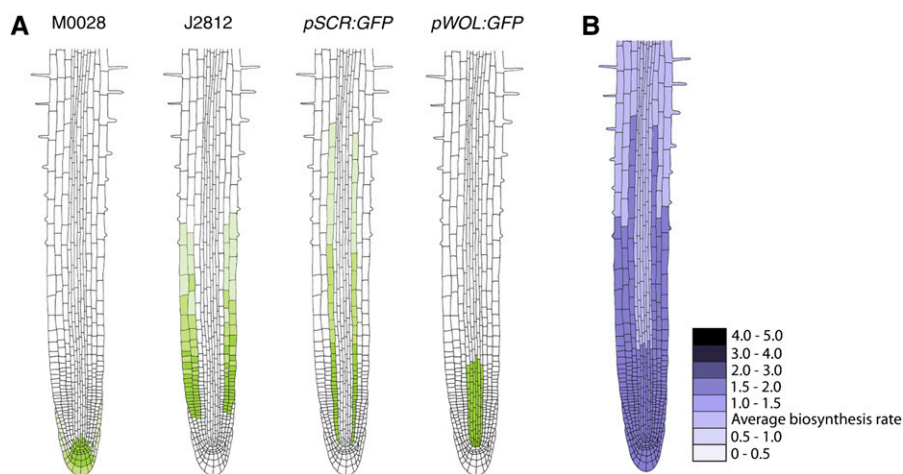


Figure 5. IAA Biosynthesis Rates Are Elevated in the *Arabidopsis* Root Apex.

(A) The GFP-expressing *Arabidopsis* lines M0028, J2812, *pSCR:GFP*, and *pWOL:GFP* were used in this study. The localization of GFP expression is indicated in green for each line.

(B) Roots were incubated for 16 h in liquid medium containing 30% $^2\text{H}_2\text{O}$ and 40 μ M NPA, and IAA synthesis rates were measured after protoplast isolation and cell sorting. The IAA biosynthesis rate was 1.5 times higher than the background level in all four lines examined, but none of the four lines showed significantly higher synthesis rate than the others.

combination of transport and conjugation/catabolism. Still, differences in IAA concentration between the columella initials (that normally show the highest GUS/GFP expression) and the differentiated columella cells can't be excluded, but from our data, it is not possible to tell if an IAA gradient exists within this cell type.

The IAA distribution map shows strong similarities to the expression patterns of the widely used artificial reporter constructs *DR5:GUS* and *DR5:GFP* (Ulmasov et al., 1997; Ottenschlager et al., 2003) in some cell types. These constructs contain a synthetic auxin response element coupled to the reporter gene and have been shown to respond to changes in IAA concentration. They display specific GUS/GFP expression patterns in the *Arabidopsis* seedling without IAA treatment, and in the root apex these lines show maximum auxin responsiveness in the QC cells. For some cell types, including the columella cells, the direct IAA quantifications indicate a lower IAA concentration than what would have been expected from previous *DR5* reporter expression data. Other commonly used auxin response reporters, such as *IAA2:GUS* (Swarup et al., 2001, 2005), *GH3:GUS* (Larkin et al., 1996), and *SAUR:GUS* (Li et al., 1991), are expressed in different cell types but also display generally elevated expression within the root apex. Immunolocalization of IAA has also been used to monitor IAA distribution within the root apex (Benkova et al., 2003), but this technique is not optimal for the cellular localization of small molecules (Ljung et al., 2004). Reporter gene and immunolocalization studies do not monitor absolute IAA concentrations within cells and tissues, but, in combination with our direct quantification of intracellular IAA concentrations and the

mathematical models recently published that attempt to describe IAA transport and distribution within the root apex (Kramer, 2004; Swarup et al., 2005; Grieneisen et al., 2007; Jones et al., 2009), we are now coming closer to being able to understand auxin dynamics and its role in root growth and development. Still, it is important to remember that with this novel technique we are measuring steady state levels of IAA within individual cell types. The future goal will be to get a better understanding of metabolic fluxes within the IAA biosynthetic and metabolic pathways, as well as monitoring IAA transport on the cellular and subcellular level.

Direct IAA synthesis measurements have previously shown that IAA sources exist within the *Arabidopsis* root (Ljung et al., 2005). Here, we demonstrate that the root apex, predominantly the zone of dividing cells, displays higher IAA synthesis rates compared with more mature tissues (Figure 5). Our measurements are supported by the findings that many putative IAA biosynthesis genes in the Trp-dependent pathways are strongly expressed in various root tissues and cell types but show strongest expression in the zone of cell division in the root tip (Table 2). Recent data show that expression of *pTAA1:GFP* in the root is localized mainly to the QC (Stepanova et al., 2008), although the cell type-specific array data suggest that the expression is much broader (Table 2). Other putative IAA synthesis genes, such as *CYP79B2*, *CYP79B3*, *ASA1*, and *ASB1* (Table 2), show strong GUS reporter gene expression within the root meristem (Ljung et al., 2005; Ikeda et al., 2009). IAA synthesis in the root apex is likely to be important for specific

Table 2. Expression of Putative IAA Biosynthesis Genes in *Arabidopsis* Root Tissues

At Code	Gene	Root Tissue								
		Lateral Root	Root Tip	Elong. Zone	Root Hair Zone	Endodermis	Endod. +cortex	Epid. Atrichoblasts	Lat. Root Cap	Stele
At5g05730	<i>ASA1/TRP5/WEI2/TIR7</i>	1,574	4,767	1,546	1,221	2,723	3,334	1,557	6,137	1,897
At2g29690	<i>ASA2</i>	98	1,420	593	411	405	598	439	392	447
At1g25220	<i>ASB1/TRP4/WEI7</i>	2,694	2,528	2,411	1,443	6,667	5,985	2,694	9,090	2,698
At5g17990	<i>PAT1/TRP1</i>	1,995	3,097	2,277	2,240	4,634	2,197	1,534	1,790	1,626
At1g29410	<i>PAI3</i>	917	2,709	1,288	1,293	1,269	1,344	1,099	1,487	1,062
At2g04400	<i>IGPS</i>	2,012	5,005	2,657	2,397	2,934	3,723	2,038	1,936	2,402
At3g54640	<i>TSA1/TRP3</i>	4,768	3,213	4,508	1,860	3,764	4,079	3,436	2,272	3,190
At4g27070	<i>TSB2</i>	6,754	12,335	7,025	8,704	13,023	8,800	4,664	10,565	4,983
At4g39950	<i>CYP79B2</i>	5,062	3,383	3,087	975	2,487	9,451	393	7,782	1,392
At2g22330	<i>CYP79B3</i>	1,666	587	911	362	467	4,666	198	1,377	457
At4g32540	<i>YUCCA</i>	253	280	209	238	242	197	185	307	362
At4g13260	<i>YUCCA2</i>	694	391	509	430	517	370	318	316	326
At1g04610	<i>YUCCA3</i>	658	3,988	715	1,983	728	2,613	1,154	4,333	1,368
At5g43890	<i>YUCCA5</i>	315	181	365	692	516	789	1,942	691	1,396
At1g70560	<i>TAA1</i>	386	944	1,327	863	1,298	1,405	1,879	1,059	2,488
At5g20960	<i>AAO1</i>	4069	2987	3520	4766	2352	4335	740	2625	2827
At1g08980	<i>AMI1</i>	987	180	292	347	273	282	224	266	178
At3g44310/300	<i>NIT1/NIT2</i>	8795	5150	7564	6387	4090	8402	8124	1873	4542
At3g44320	<i>NIT3</i>	3181	2851	5692	2714	7620	4758	5453	6255	2161
At5g22300	<i>NIT4</i>	379	466	348	368	402	339	462	319	397

The data were extracted from tissue and cell type-specific (Birbaum et al., 2003) microarray data using the Genevestigator tool (<https://www.genevestigator.ethz.ch/>; Zimmermann et al., 2005). These genes have all been described by Woodward and Bartel (2005) except for *TAA1* (Stepanova et al., 2008; Tao et al., 2008).

developmental processes in the root, such as cell elongation (Swarup et al., 2007), polar root hair positioning (Ikeda et al., 2009), and lateral root initiation (Casimiro et al., 2001). The possibility of multiple pathways operating in the root apex (Woodward and Bartel, 2005), perhaps with specific roles during development and perhaps also with different subcellular localization, is intriguing, and further development in analytical MS technology will hopefully make it possible to analyze IAA synthesis rates with even higher resolution.

In this study, we have established new tools to unravel the role of IAA transport versus local IAA synthesis in the formation of gradients and concentration maxima of IAA, contributing to specific developmental processes within the root apex. The combined application of FACS and MS technologies established here will likely aid future analyses of the cellular distribution and production patterns of hormones and other regulatory molecules in diverse multicellular organisms.

METHODS

Plant Material and Growth Conditions

Arabidopsis thaliana seeds (GFP lines *PET111:GFP*, *pWOODEN LEG:GFP* [*pWOL:GFP*], *pWERWOLF:GFP* [*pWER:GFP*], *pSCARECROW:GFP* [*pSCR:GFP*], J2812, J3411, J0571, J2501, Q0990, J0121, M0028, J0951, *pAGAMOUS LIKE 42:GFP* [*pAGL42:GFP*], and *DR5:GFP*; see Supplemental Table 1 and Supplemental Figure 1 online) were surface-sterilized by treatment first with a mixture of 70% ethanol and 0.1% Tween and then with 95% ethanol. After 3 d of vernalization, seeds were sown on agar plates (30 mM sucrose, 4.4 g Murashige and Skoog medium, 2.6 mM MES, and 1% agar, pH 5.7) covered with a nylon mesh (Sefar Nitex 03-110/47) and placed vertically for 8 d in long-day conditions (16 h light and 8 h darkness) and at a temperature of 23°C.

Protoplast Isolation

Pectolyase (Sigma-Aldrich P-5936) and cellulysin (Calbiochem 219466) were dissolved in protoplast isolation buffer (600 mM mannitol, 2 mM MgCl₂, 0.1% BSA, 2 mM CaCl₂, 2 mM MES, and 10 mM KCl, pH 5.7) to a final concentration of 45 units/mL cellulysin and 0.3 units/mL pectolyase. The apical part of the root (approximately one-third of the total root length) was collected and incubated in the resulting buffer for 2 h in 22°C with gentle stirring (110 rpm). Remaining tissue was removed by filtration through a 40- μ m cell strainer (Becton, Dickinson and Company). Protoplasts were centrifuged at 1000 Relative Centrifugal Force (Hettich Universal 32), resuspended in PBS buffer (0.15 M NaCl, 8 mM Na₂HPO₄, 2.7 mM KCl, and 1.47 mM KH₂PO₄, pH 7.4) and kept on ice until sorted.

Cell Size Measurements

The diameter of isolated protoplasts was measured using a Zeiss Axioplan 2 microscope. The size of the GFP-expressing cells in the different *Arabidopsis* lines was measured using CLSM. Roots were counterstained with propidium iodide, rinsed, and mounted in water. Confocal images were obtained using LSM50 (Zeiss) and TCS SP2 (Leica) confocal microscopes with $\times 20$ and $\times 40$ water immersion objectives. An Ar/Kr 488-nm laser was used for excitation. GFP emission was detected using a 505- to 530-nm emission filter and propidium iodide emission with a 560-nm filter. Three-dimensional images of root cells were reconstructed from 40 to 60 optical 1- μ m sections obtained at 0.5- μ m intervals using an LSM Image Analyzer (Zeiss). To calculate the cell volumes,

multipoint measurement of the areas and lengths in z-stacks of 10 cells were obtained.

Leakage Tests

Protoplasts were isolated as described above with or without 40 μ M NPA, 30 μ M 1-NOA, or 0.02% NaN₃ (w/v) added to the isolation buffer. Isolated protoplasts were suspended in BD FACSFlow buffer (Becton, Dickinson and Company) and either analyzed directly or left on ice for 0 to 170 min to simulate the sorting procedure. Samples were taken at six different time points and centrifuged for 3 min at 1000 Relative Centrifugal Force, and the IAA concentration in the protoplast pellets and supernatants was analyzed as described below.

Cell Sorting

Cell sorting was performed using a FACSVantage Flow Cytometer/Cell Sorter equipped with a 100- μ m nozzle (Becton, Dickinson and Company) as previously described (Birnbaum et al., 2003, 2005). Intact root protoplasts were identified using forward and side scatter signals, and GFP-positive and -negative protoplasts were separated according to their GFP emission and autofluorescence after excitation by the 488-nm laser. Data were processed using FACSDiVa 5.0 software. The samples were kept on ice prior to and after sorting (which was performed after cooling the samples to 4°C).

IAA Quantification

Aliquots of around 150,000 protoplasts suspended in BD FACSFlow buffer (Becton, Dickinson and Company) were used for each technical replicate. Prior to extraction, 125 pg ¹³C₆-IAA internal standard was added to each sample, which was then frozen to rupture the plasma membranes of the cells. IAA was then purified by acidifying the samples to pH 2.7 with 1 M HCl, applying them at a rate of 1 mL/min to a 50-mg C18 Bond Elute SPE column (Varian) conditioned with 1 mL methanol and 1 mL 1% acetic acid, washing with 1 mL 10% methanol in 1% acetic acid, and eluting with 1 mL methanol. After evaporation to dryness, each sample was methylated by adding 0.2 mL 2-propanol, 1 mL methyl chloride, and 5 μ L trimethylsilyl-diazomethane in hexane and then incubating for 30 min at room temperature. Five microliters of 2 M acetic acid in hexane was added to destroy excess diazomethane in each sample, which was subsequently evaporated to dryness. After trimethylsilylation, IAA was quantified using GC-SRM-MS as described by Edlund et al. (1995).

IAA Biosynthesis Measurements

Excised roots from the GFP lines M0028, J2812, *pSCR:GFP*, and *pWOL:GFP*, grown as described above, were incubated for 16 h in liquid medium containing 30 mM sucrose, 4.4 g Murashige and Skoog medium, 2.6 mM MES, 30% ²H₂O, and 40 μ M NPA, pH 5.7. After incubation, protoplasts were isolated and sorted by FACS, and IAA was then extracted and purified from the GFP and non-GFP protoplast fractions as described above. IAA synthesis rates were measured by GC-SRM-MS as described by Ljung et al. (2005).

Metabolite Profiling of Isolated Protoplasts

A part of each sample prepared for IAA quantification was also subjected to metabolite profiling using a Pegasus III gas chromatograph-time of flight-mass spectrometer (Leco) as described by Jonsson et al. (2005). One microliter (1/20) was injected splitless into an Agilent 6890 GC equipped with a 10 m \times 0.18 mm i.d. DB 5-MS capillary column with

0.18- μm stationary phase (J and W Scientific). Ions were generated by a 70-eV electron beam at an ionization current of 2.0 mA, and 30 spectra s^{-1} were recorded in the mass range 50 to 800 m/z with unit resolution. Data were processed according to Jonsson et al. (2005) and evaluated by PCA.

Identification of IAA Metabolites in Isolated Protoplasts

Wild-type *Arabidopsis* Columbia seedlings were grown for 7 d in long days as described by Ljung et al. (2005). Intact seedlings (five to seven, 0.7 to 1.2 g fresh weight) were incubated with 0.75 mL sterile Murashige and Skoog medium containing 1 μM [$1\text{'-}^{14}\text{C}$]-IAA (American Radiolabeled Chemicals) for 8 h. For incubations of roots, the aerial parts of the seedlings were removed with a scalpel, and $\sim 1\ \mu\text{g}$ (0.3 μCi) of [$1\text{'-}^{14}\text{C}$]-IAA dissolved in 0.5 mL of sterile 0.3% agar was applied just above the cutting line. After 8 h, roots tips ($\sim 5\ \text{mm}$) were collected and washed with distilled water, and protoplasts were isolated as described above. Samples of intact roots were prepared as well as whole seedlings. Whole seedlings and intact roots were homogenized using a Retsch Mixer Mill in 1 mL of ice-cold 50 mM phosphate buffer, pH 7. Protoplast samples were sonicated for 3 min in the protoplast preparation buffer using a T460 sonicator (ELMA). Samples were then acidified and purified using 50-mg C18 Bond Elut SPE columns as described above. After purification, samples were evaporated and dissolved in 100 μL of 10% methanol. An aliquot of each sample, containing $\sim 0.05\ \mu\text{Ci}$, was injected, and HPLC analysis combined with radioactive scintillation counting was performed as described by Östin et al. (1998). For samples containing low amounts of radioactivity, 1-min fractions were collected and their radioactivity was measured using a Beckman LS6500 scintillation counter (Beckman Coulter).

Author Contributions

G.S. and P.N.B. conceived the project. K.L., S.V.P., G.S., J.Y.W., and P.N.B. designed, performed, and analyzed the cell sorting/MS experiments. S.V.P., A.I.J., M.K., and T.M. designed, performed, and analyzed the IAA metabolism experiments. A.M. and M.G. performed the cell size measurements using CLSM. K.L., S.V.P., and G.S. wrote the manuscript. All authors contributed to the interpretation of results and edited the manuscript.

Supplemental Data

The following materials are available in the online version of this article.

Supplemental Figure 1. GFP Reporter Gene Expression.

Supplemental Figure 2. PCA of Metabolite Profiles from Isolated Protoplasts.

Supplemental Table 1. *Arabidopsis* GFP Lines Used for Cell Sorting.

ACKNOWLEDGMENTS

The Nottingham Arabidopsis Stock Centre provided the GAL4-GFP enhancer trap lines from the Jim Haseloff collections, and some of the GFP constructs used in this study were kind gifts from Ben Scheres and Klaus Palme. We thank Roger Granbom, Gun Lövdahl, Ilkka Sairanen, and Åsa Larefalk for technical assistance with FACS and MS analyses. We also thank Brian Jones, Ben Scheres, and Veronica Grieneisen for fruitful discussions and helpful comments on the manuscript. The work was supported by the Swedish Research Council (G.S. and K.L.) and the National Science Foundation AT2010 program (P.N.B.).

Received February 20, 2009; revised May 4, 2009; accepted May 12, 2009; published June 2, 2009.

REFERENCES

- Benfey, P.N., and Scheres, B. (2000). Root development. *Curr. Biol.* **10**: R813–R815.
- Benjamins, R., and Scheres, B. (2008). Auxin, the looping star in plant development. *Annu. Rev. Plant Biol.* **59**: 443–465.
- Benková, E., Michniewicz, M., Sauer, M., Teichmann, T., Seifertová, D., Jürgens, G., and Friml, J. (2003). Local, efflux-dependent auxin gradients as a common module for plant organ formation. *Cell* **115**: 591–602.
- Bhalerao, R.P., and Bennett, M.J. (2003). The case for morphogens in plants. *Nat. Cell Biol.* **5**: 939–943.
- Bhalerao, R.P., Eklöf, J., Ljung, K., Marchant, A., Bennett, M., and Sandberg, G. (2002). Shoot-derived auxin is essential for early lateral root emergence in *Arabidopsis* seedlings. *Plant J.* **29**: 325–332.
- Birnbaum, K., Jung, J.W., Wang, J.Y., Lambert, G.M., Hirst, J.A., Galbraith, D.W., and Benfey, P.N. (2005). Cell type-specific expression profiling in plants via cell sorting of protoplasts from fluorescent reporter lines. *Nat. Methods* **2**: 615–619.
- Birnbaum, K., Shasha, D.E., Wang, J.Y., Jung, J.W., Lambert, G.M., Galbraith, D.W., and Benfey, P.N. (2003). A gene expression map of the *Arabidopsis* root. *Science* **302**: 1956–1960.
- Blakeslee, J.J., Peer, W.A., and Murphy, A.S. (2005). Auxin transport. *Curr. Opin. Plant Biol.* **8**: 494–500.
- Brady, S.M., Orlandy, D.A., Lee, J.-Y., Wang, J.Y., Koch, J., Dinneny, J.R., Mace, D.M., Ohler, U., and Benfey, P.N. (2007). A high-resolution root spatiotemporal map reveals dominant expression patterns. *Science* **318**: 801–806.
- Caruso, J., Pence, V., and Leverone, L. (1995). Immunoassay methods of plant hormone analysis. In *Plant Hormones: Physiology, Biochemistry and Molecular Biology*, P.J. Davies, ed, 2nd ed. (Norwell, MA: Kluwer Academic Publishers), pp. 433–447.
- Casimiro, I., Marchant, A., Bhalerao, R.P., Beeckman, T., Dhooge, S., Swarup, R., Graham, N., Inzé, D., Sandberg, G., Casero, P.J., and Bennett, M. (2001). Auxin transport promotes *Arabidopsis* lateral root initiation. *Plant Cell* **13**: 843–852.
- Chen, R., Hilson, P., Sedbrook, J., Rosen, E., Caspar, T., and Masson, P.H. (1998). The *Arabidopsis thaliana* *AGRAVITROPIC 1* gene encodes a component of the polar-auxin-transport efflux carrier. *Proc. Natl. Acad. Sci. USA* **95**: 15112–15117.
- Edlund, A., Eklöf, S., Sundberg, B., Moritz, T., and Sandberg, G. (1995). A microscale technique for gas chromatography-mass spectrometry measurements of picogram amounts of indole-3-acetic acid in plant tissues. *Plant Physiol.* **108**: 1043–1047.
- Grieneisen, V.A., Xu, J., Marée, A.F., Hogeweg, P., and Scheres, B. (2007). Polar transport is sufficient to generate a maximum and gradient guiding root growth. *Nature* **449**: 1008–1013.
- Ikeda, Y., Men, S., Fischer, U., Stepanova, A.N., Alonso, J.M., Ljung, K., and Grebe, M. (May 17, 2009). Local auxin biosynthesis modulates gradient-directed planar polarity in *Arabidopsis*. *Nat. Cell Biol.*, (online) doi:10.1038/ncb1879.
- Jones, A.R., Kramer, E.M., Knox, K., Swarup, R., Bennett, M.J., Lazarus, C.M., Leyser, H.M., and Grierson, C.S. (2009). Auxin transport through non-hair cells sustains root-hair development. *Nat. Cell Biol.* **11**: 78–84.
- Jonsson, P., Johansson, A.I., Gullberg, J., Trygg, J., Jiye, A., Grung, B., Marklund, S., Sjöström, M., Antti, H., and Moritz, T. (2005). High-throughput data analysis for detecting and identifying differences between samples in GC/MS-based metabolomic analyses. *Anal. Chem.* **77**: 5635–5642.
- Kramer, E.M. (2004). PIN and AUX/LAX proteins: Their role in auxin accumulation. *Trends Plant Sci.* **9**: 578–582.
- Larkin, P.J., Gibson, J.M., Mathesius, U., Weinman, J.J., Gartner, E.,

- Hall, E., Tanner, G.J., Rolfe, B.G., and Djordjevic, M.A. (1996). Transgenic white clover. Studies with the auxin-responsive promoter, GH3, in root gravitropism and lateral root development. *Transgenic Res.* **5**: 325–335.
- Leyser, O. (2006). Dynamic integration of auxin transport and signaling. *Curr. Biol.* **6**: R424–R433.
- Li, Y., Hagen, G., and Guilfoyle, T.J. (1991). An auxin-responsive promoter is differentially induced by auxin gradients during tropisms. *Plant Cell* **11**: 1167–1175.
- Ljung, K., Bhalerao, R.P., and Sandberg, G. (2001). Sites and homeostatic control of auxin biosynthesis in *Arabidopsis* during vegetative growth. *Plant J.* **28**: 465–474.
- Ljung, K., Hull, A.K., Celenza, J., Yamada, M., Estelle, M., Normanly, J., and Sandberg, G. (2005). Sites and regulation of auxin biosynthesis in *Arabidopsis* roots. *Plant Cell* **17**: 1090–1104.
- Ljung, K., Sandberg, G., and Moritz, T. (2004). Methods of plant hormone analysis. In *Plant Hormones: Biosynthesis, Signal Transduction, Action!* P.J. Davies, ed, 3rd ed. (Kluwer Academic Publishers, Norwell, MA, USA), pp. 671–694.
- Lawy, T., Lee, J.-Y., Colinas, J., Wang, J.Y., Thongrod, S.C., Malamy, J.E., Birnbaum, K., and Benfey, P.N. (2005). Transcriptional profile of the *Arabidopsis* root quiescent center. *Plant Cell* **17**: 1908–1925.
- Östin, A., Kowalczyk, M., Bhalerao, R.P., and Sandberg, G. (1998). Metabolism of indole-3-acetic acid in *Arabidopsis*. *Plant Physiol.* **118**: 285–296.
- Ottenschläger, I., Wolff, P., Wolverton, C., Bhalerao, R.P., Sandberg, G., Ishikawa, H., Evans, M., and Palme, K. (2003). Gravity-regulated differential auxin transport from columella to lateral root cap cells. *Proc. Natl. Acad. Sci. USA* **100**: 2987–2991.
- Parry, G., Delbarre, A., Marchant, A., Swarup, R., Napier, R., Perrot-Rechenmann, C., and Bennett, M.J. (2001). Novel auxin transport inhibitors phenocopy the auxin influx carrier mutation *aux1*. *Plant J.* **25**: 399–406.
- Petrasek, J., et al. (2006). PIN proteins perform a rate-limiting function in cellular auxin efflux. *Science* **312**: 914–918.
- Prusinkiewicz, P., and Rolland-Lagan, A.G. (2006). Modeling plant morphogenesis. *Curr. Opin. Plant Biol.* **9**: 83–88.
- Sabatini, S., Beis, D., Wolkenfelt, H., Murfett, J., Guilfoyle, T., Malamy, J., Benfey, P., Leyser, O., Bechtold, N., Weisbeek, P., and Scheres, B. (1999). An auxin-dependent distal organizer of pattern and polarity in the *Arabidopsis* root. *Cell* **24**: 463–472.
- Sandberg, G., Gardeström, P., Sitbon, F., and Olsson, O. (1990). Presence of indole-3-acetic acid in chloroplasts of *Nicotiana tabacum* and *Pinus sylvestris*. *Planta* **180**: 562–568.
- Stepanova, A.N., Robertson-Hoyt, J., Yun, J., Benavente, L.M., Xie, D.Y., Dolezal, K., Schlereth, A., Jürgens, G., and Alonso, J.M. (2008). TAA1-mediated auxin biosynthesis is essential for hormone crosstalk and plant development. *Cell* **133**: 31–32.
- Suga, S., Murai, M., Kuwagata, T., and Maeshima, M. (2003). Differences in aquaporin levels among cell types of radish and measurement of osmotic water permeability of individual protoplasts. *Plant Cell Physiol.* **44**: 277–286.
- Swarup, R., Friml, J., Marchant, A., Ljung, K., Sandberg, G., Palme, K., and Bennett, K. (2001). Localization of the auxin permease AUX1 suggests two functionally distinct hormone transport pathways operate in the *Arabidopsis* root apex. *Genes Dev.* **15**: 2648–2653.
- Swarup, R., Kramer, E.M., Perry, P., Knox, K., Leyser, H.M.O., Haseloff, J., Beemster, G.T.S., Bhalerao, R., and Bennett, M.J. (2005). Root gravitropism requires lateral root cap and epidermal cells for transport and response to a mobile auxin signal. *Nat. Cell Biol.* **7**: 1057–1065.
- Swarup, R., Perry, P., Hagenbeek, D., Van Der Straeten, D., Beemster, G.T.S., Sandberg, G., Bhalerao, R., Ljung, K., and Bennett, M.J. (2007). Ethylene upregulates auxin biosynthesis in *Arabidopsis* seedlings to enhance inhibition of root cell elongation. *Plant Cell* **19**: 2186–2196.
- Tanaka, H., Dhonukshe, P., Brewer, P.B., and Friml, J. (2006). Spatiotemporal asymmetric auxin distribution: a means to coordinate plant development. *Cell. Mol. Life Sci.* **63**: 2738–2754.
- Tao, Y., et al. (2008). Rapid synthesis of auxin via a new tryptophan-dependent pathway is required for shade avoidance in plants. *Cell* **133**: 164–176.
- Tucker, E.B. (1993). Azide treatment enhances cell-to-cell diffusion in staminal hairs of *Setcreasea purpurea*. *Protoplasma* **17**: 45–49.
- Uggle, C., Moritz, T., Sandberg, G., and Sundberg, B. (1996). Auxin as a positional signal in pattern formation in plants. *Proc. Natl. Acad. Sci. USA* **93**: 9282–9286.
- Ulmasov, T., Murfett, J., Hagen, G., and Guilfoyle, T. (1997). Aux/IAA proteins repress expression of reporter genes containing natural and highly active synthetic auxin response elements. *Plant Cell* **9**: 1963–1971.
- Woodward, A.W., and Bartel, B. (2005). Auxin: Regulation, action, and interaction. *Ann. Bot. (Lond.)* **95**: 707–735.
- Wright, K.M., and Oparka, K.J. (1997). Metabolic inhibitors induce symplastic movement of solutes from the transport phloem of *Arabidopsis* roots. *J. Exp. Bot.* **48**: 1807–1814.
- Zimmermann, P., Hennig, L., and Grissem, W. (2005). Gene expression analysis and network discovery using Genevestigator. *Trends Plant Sci.* **10**: 407–409.